Suppression of long-range collective effects in meta-surfaces formed by plasmonic antenna pairs

S. Hossein Mousavi,[1,8] Alexander B. Khanikaev,[1,8] Burton Neuner III,[1] David Y. Fozdar,[1] Timothy D. Corrigan,[2] Paul W. Kolb,[3] H. Dennis Drew,[3–5] Raymond J. Phaneuf,[3–6] Andrea Alù,[7] and Gennady Shvets[1,*]

[1]*Department of Physics, The University of Texas at Austin, Austin, TX 78712, USA*
[2]*Department of Physical Sciences, Concord University, Athens, WV 24712, USA*
[3]*Laboratory for Physical Sciences, College Park, MD 20740, USA*
[4]*Department of Physics, University of Maryland, College Park, MD 20742, USA*
[5]*Center for Nanoscale and Advanced Materials, University of Maryland, College Park, MD 20742, USA*
[6]*Department of Material Science and Engineering, University of Maryland, College Park, MD 20742, USA*
[7]*Department of Electrical and Computer Engineering, The University of Texas at Austin, Austin, TX 78712, USA*
[8] *These authors contributed equally to this work.*
**gena@physics.utexas.edu*

Abstract: The collective effects in a periodic array of plasmonic double-antenna meta-molecules are studied. We experimentally observe that the collective behavior in this structure substantially differs from the one observed in their single-antenna counterparts. This behavior is explained using an analytical dipole model. We find that in the double-antenna case the effective dipole-dipole interaction is significantly modified and the transverse long-range interaction is suppressed, giving rise to the disappearance of Wood's anomalies. Numerical calculations also show that such suppression of long-range interaction results in an anomalous spatial dispersion of the electric-dipolar mode, making it insensitive to the angle of incidence. In contrast, the quadrupolar mode of the antenna pair experiences strong spatial dispersion. These results show that collective effects in plasmonic metamaterials are very sensitive to the design and topology of meta-molecules. Our findings envision the possibility of suppressing the spatial dispersion effects to weaken the dependence of the metamaterials' response on the incidence angle.

OCIS codes: (250.5403) Plasmonics; (160.3918) Metamaterials; (240.6680) Surface plasmons; (310.6628) Subwavelength structures, nanostructures; (350.4238) Nanophotonics and photonic crystals.

References and links

1. W. L. Barnes, A. Dereux, and T. W. Ebbesen, "Surface plasmon subwavelength optics," Nature (London) **424**, 824–830 (2003).
2. H. A. Atwater and A. Polman, "Plasmonics for improved photovoltaic devices," Nature Mater. **9**, 205–213 (2010).
3. N. Liu, M. L. Tang, M. Hentschel, H. Giessen, and A. P. Alivisatos, "Nanoantenna-enhanced gas sensing in a single tailored nanofocus," Nat. Mater. **10**, 631–636 (2011).

#151537 - $15.00 USD Received 22 Jul 2011; revised 15 Sep 2011; accepted 16 Sep 2011; published 24 Oct 2011

4. R. Adato, A. A. Yanik, J. J. Amsden, D. L. Kaplan, F. G. Omenetto, M. K. Hong, S. Erramilli, and H. Altug, "Ultra-sensitive vibrational spectroscopy of protein monolayers with plasmonic nanoantenna arrays," Proc. Natl Acad. Sci. U.S.A. **106**, 19227–19232 (2009).
5. A. Yanik, A. Cetin, M. Huang, A. Artar, S. H. Mousavi, A. B. Khanikaev, J. Connor, G. Shvets, and H. Altug, "Seeing protein monolayers with naked eye through plasmonic Fano resonances," Proc. Natl Acad. Sci. U.S.A. **108**, 11784–11789 (2011).
6. S. Lal, S. Link, and N. J. Halas, "Nano-optics from sensing to waveguiding," Nat. Photon. **1**, 641–648 (2007).
7. T. W. Ebbesen, H. J. Lezec, H. F. Ghaemi, T. Thio, and P. A. Wolff, "Extraordinary optical transmission through sub-wavelength hole arrays," Nature (London) **391**, 667–669 (1998).
8. L. Martín-Moreno, F. J. García-Vidal, H. J. Lezec, K. M. Pellerin, T. Thio, J. B. Pendry, and T. W. Ebbesen, "Theory of extraordinary optical transmission through subwavelength hole arrays," Phys. Rev. Lett. **86**, 1114–1117 (2001).
9. W. H. Weber and G. W. Ford, "Propagation of optical excitations by dipolar interactions in metal nanoparticle chains," Phys. Rev. B **70**, 125429 (2004).
10. B. Auguié, and W. L. Barnes, "Collective resonances in gold nanoparticle arrays," Phys. Rev. Lett. **101**, 143902 (2008).
11. G. Vecchi, V. Giannini, and J. Gómez Rivas, "Surface modes in plasmonic crystals induced by diffractive coupling of nanoantennas," Phys. Rev. B **80**, 201401 (2009).
12. J. B. Pendry, L. Martín-Moreno, and F. J. García-Vidal, "Mimicking surface plasmons with structured surfaces," Science **305**, 847–848 (2004).
13. F. J. García de Abajo and J. J. Sáenz, "Electromagnetic surface modes in structured perfect-conductor surfaces," Phys. Rev. Lett. **95**, 233901 (2005).
14. S. H. Mousavi, A. B. Khanikaev, B. Neuner III, Y. Avitzour, D. Korobkin, G. Ferro, and G. Shvets, "Highly confined hybrid spoof surface plasmons in ultrathin metal-dielectric heterostructures," Phys. Rev. Lett. **105**, 176803 (2010).
15. S. Zou, N. Janel, and G. C. Schatz, "Silver nanoparticle array structures that produce remarkably narrow plasmon lineshapes," J. Chem. Phys. **120**, 10871–10875 (2004).
16. S. Zou and G. C. Schatz, "Narrow plasmonic/photonic extinction and scattering line shapes for one and two dimensional silver nanoparticle arrays," J. Chem. Phys. **121**, 12606–12612 (2004).
17. W. Zhou, and T. W. Odom, "Tunable subradiant lattice plasmons by out-of-plane dipolar interactions," Nat Nano **6**, 423–427 (2011).
18. Y. Chu, E. Schonbrun, T. Yang, and K. B. Crozier, "Experimental observation of narrow surface plasmon resonances in gold nanoparticle arrays," Appl. Phys. Lett. **93**, 181108 (2008).
19. V.G. Kravets, F. Schedin, and A. N. Grigorenko, "Extremely Narrow Plasmon Resonances Based on Diffraction Coupling of Localized Plasmons in Arrays of Metallic Nanoparticles," Phys. Rev. Lett. **101**, 087403 (2008).
20. A. Alù, and N. Engheta, "Theory of linear chains of metamaterial/plasmonic particles as subdiffraction optical nanotransmission lines," Phys. Rev. B **74**, 205436 (2006).
21. F. J. García de Abajo, "Light scattering by particle and hole arrays," Rev. Mod. Phys. **79**, 1267–1290 (2007).
22. R. W. Wood, "Films of minute metallic particles," Phil. Mag. **4**, 396 (1902).
23. P. W. Kolb, T. D. Corrigan, H. D. Drew, A. B. Sushkov, R. J. Phaneuf, A. Khanikaev, S. H. Mousavi, and G. Shvets, "Bianisotropy and spatial dispersion in highly anisotropic near-infrared resonator arrays," Opt. Express **18**, 24025–24036 (2010).
24. J. Aizpurua, G. W. Bryant, L. J. Richter, and F. J. García de Abajo, "Optical properties of coupled metallic nanorods for field-enhanced spectroscopy," Phys. Rev. B **71**, 235420 (2005).
25. L. Novotny, "Effective wavelength scaling for optical antennas," Phys. Rev. Lett. **98**, 266802 (2007).
26. N. Liu, L. Langguth, T. Weiss, J. Kästel, M. Fleischhauer, T. Pfau, and H. Giessen, "Plasmonic analogue of electromagnetically induced transparency at the Drude damping limit," Nat. Mater. **8**, 758-762 (2009).
27. C. Wu, A. B. Khanikaev, and G. Shvets, "Broadband slow light metamaterial based on a double-continuum Fano resonance," Phys. Rev. Lett. **106**, 107403 (2011).
28. K. Kempa, R. Ruppin, and J. B. Pendry, "Electromagnetic response of a point-dipole crystal," Phys.Rev. B **72**, 205103 (2005).
29. D. H. Dawes, R. C. McPhedran, and L. B. Whitbourn, "Thin capacitive meshes on a dielectric boundary: theory and experiment," Appl. Opt. **28**, 3498–3510 (1989).
30. A. Alù, and N. Engheta, "Guided Propagation along Quadrupolar Chains of Plasmonic Nanoparticles," Phys. Rev. B **79**, 235412 (2009).
31. A. Alù and N. Engheta, "Dynamical theory of artificial optical magnetism produced by rings of plasmonic nanoparticles," Phys. Rev. B **78**, 085112 (2008).
32. A. B. Khanikaev, S. H. Mousavi, G. Shvets, and Y. S. Kivshar, "One-way extraordinary optical transmission and nonreciprocal spoof plasmons," Phys. Rev. Let. **105**, 126804 (2010).
33. A. Alù and N. Engheta, "The quest for magnetic plasmons at optical frequencies," Opt. Express **17**, 5723–5730 (2009).
34. X. M. Bendana and F. J. García de Abajo, "Confined collective excitations of self-standing and supported planar

#151537 - $15.00 USD Received 22 Jul 2011; revised 15 Sep 2011; accepted 16 Sep 2011; published 24 Oct 2011

periodic particle arrays," Opt. Express **17**, 18826–18835 (2009).
35. B. Auguié, X. M. Bendaña, W. L. Barnes, and F. J. García de Abajo, "Diffractive arrays of gold nanoparticles near an interface: critical role of the substrate," Phys. Rev. B **82**, 155447 (2010).
36. G. Vecchi, V. Giannini, and J. Gómez Rivas, "Shaping the fluorescent emission by lattice resonances in plasmonic crystals of nanoantennas," Phys. Rev. Lett. **102**, 146807 (2009).
37. V. Giannini, G. Vecchi, and J. Gómez Rivas, "Lighting up multipolar surface plasmon polaritons by collective resonances in arrays of nanoantennas," Phys. Rev. Lett. **105**, 266801 (2010).

1. Introduction

The importance of metamaterials operating in the IR and visible domains for various applications, including plasmonics [1], photovoltaics and thermo-photovoltaics [2], and sensing [3, 4, 5, 6] is hard to underestimate. For this reason, the metamaterials with a resonant response at optical frequencies have recently attracted significant attention. In periodic plasmonic metamaterials, collective effects are known to play an important role, and give rise to such effects as extraordinary optical transmission (EOT) [7, 8], the formation of collective guided modes [9, 10, 11] such as spoof [12, 13] and hybrid spoof surface plasmons [14], and an increased lifetime of resonances [15, 16, 17, 18, 19].

The collective behavior in optical metamaterials originates from inherent nonlocal effects. In the case of a periodic assembly of meta-molecules, the major source of non-locality is long-range interaction [9, 10, 15, 16, 20, 21]. Collective long-range effects are most strongly manifested at the onset of Bragg diffraction, when the period is comparable to the wavelength and the correlation length effectively diverges. In this case, the long-range interaction dominates over the near-field interaction and gives rise to the appearance of Wood's anomalies [22]. Even at longer wavelengths the long-range interaction can significantly affect the optical response of metamaterials. It has long been recognized that both Wood's anomalies and the structure of the unit cell (e.g., its dipole polarizability) strongly influence metamaterial response. For example, the spectral positions of EOT maxima are influenced by the size and shape of the holes in the metal film [13, 21]. The effect of the *topology* of the unit cell, on the other hand, has not received significant attention.

In this paper, we demonstrate that collective long-range effects can be considerably reduced for unit cells comprised of a pair of disconnected antennas. We theoretically and experimentally study a meta-surface which represents a two-dimensional periodic array of double plasmonic antennas [23]. We focus on the frequency range where the individual antennas experience an electric-dipolar antenna resonance [24, 25]. The double-antenna meta-molecule represents the simplest design experiencing a quadrupolar [26, 27] resonance along with the dipolar resonance, stemming from the single-antenna resonance. When the meta-molecules are arranged to form a periodic array, the collective dipolar and quadrupolar modes emerge from the resonances of the individual meta-molecules. To analyze the collective behavior of this structure, we use a standard dipole model [15, 16, 20, 10, 21, 28]. We show that the dipole model can qualitatively describe the experimentally observed anomalous collective response of the meta-surface. These results are confirmed by a rigorous numerical modal matching technique [29].

The paper is organized as follows: in Section 2 we outline the dipole model of a single-antenna meta-surface (SAM), followed by its extension to the double-antenna meta-surface (DAM). In Section 3 we present the experimental and numerical results and explain the observed behavior applying our analytical model. The results for SAM and DAM are compared and the observed differences are discussed. Finally Section 4 summarizes our results and puts them into perspective with meta-surface applications.

#151537 - $15.00 USD Received 22 Jul 2011; revised 15 Sep 2011; accepted 16 Sep 2011; published 24 Oct 2011

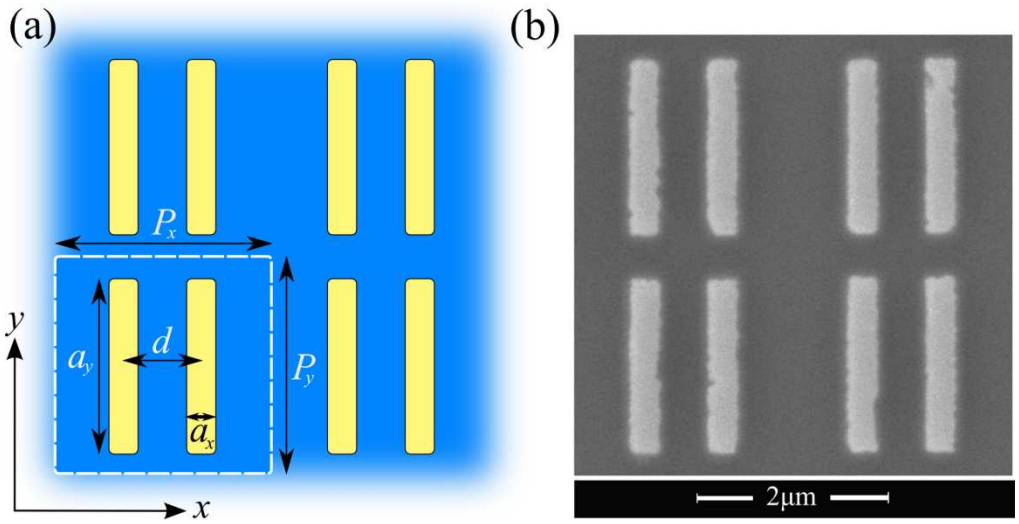

Fig. 1. (a) Schematics of a double-antenna meta-surface on a substrate. (b) SEM image of the sample grown on CaF_2 ($\varepsilon = n^2 = 1.96$). The structure dimensions are $a_y = 1.8\ \mu m$, $a_x = 0.3\ \mu m$, $P = P_x = P_y = 2.25\ \mu m$, and $d = 0.8\ \mu m$.

2. Optical response of SAM and DAM structures

To understand the physics underlying the optical properties of DAM and demonstrate the importance of the meta-molecule geometry on the collective response, we use as a reference its well-understood counterpart, which consists of periodically arranged single plasmonic antennas. In this paper, we will focus on the case of *s*-polarized incidence for which DAM and SAM exhibit a strong discrepancy and DAM experiences a quadrupolar resonance. An *s*-polarized incidence is defined by the wave-vector of the incident wave in the *xz*-plane ($k_y = 0$, $k_x \neq 0$) and the electric field along the antennas (*y* direction).

2.1. *Single-antenna meta-surface*

First, we outline the dipole model, commonly used to describe collective effects in plasmonic metamaterials [15, 16, 20, 10, 21, 28, 30, 31]. In its simplest version, the dipole model treats each meta-molecule with a finite size as a point electric-dipole $\mathbf{p}$ with a polarizability α relating the local electric field $\mathbf{E}_{\rm loc}$ to the dipole moment, $\mathbf{p} = \alpha(\omega)\mathbf{E}_{\rm loc}$. The local electric field polarizing the dipole at the position $\mathbf{r}$ is the superposition of the incident electric field and the electric field scattered by the other dipoles in the assembly, $\mathbf{E}_{\rm loc}(\mathbf{r}) = \mathbf{E}_{\rm ext}(\mathbf{r}) + \sum_{m\neq 0}\mathbf{E}_m(\mathbf{r})$, where the sum excludes the self-interaction, $\mathbf{E}_m(\mathbf{r}) = \hat{g}(\mathbf{R}_m - \mathbf{r})\exp[-i\mathbf{k}_{\|}\cdot(\mathbf{R}_m - \mathbf{r})]\mathbf{p}$, $\hat{g}(\mathbf{r}) = (\nabla\nabla + k^2)\exp(ikr)/r$ is the dipole-dipole interaction tensor, $k = n\omega/c$ where $n = \sqrt{\varepsilon}$ stands for the refractive index, $\mathbf{k}_{\|} = (k_x, k_y)$ is the in-plane wave-vector, and $\mathbf{R}_m$ is the position of the *m*-th dipole in the array. By assuming that the antennas are polarizable only along the *y* direction,

#151537 - $15.00 USD Received 22 Jul 2011; revised 15 Sep 2011; accepted 16 Sep 2011; published 24 Oct 2011

one can obtain the effective polarizability of the dipole in the array,

$$\alpha_{\text{eff}}(\mathbf{k}_\parallel,\omega)=\frac{1}{\alpha^{-1}(\omega)-S_0(\mathbf{k}_\parallel,\omega)},$$
$$S_0(\mathbf{k}_\parallel,\omega)=\sum_{m\neq 0} g_{yy}(\mathbf{R}_m)\exp(-i\mathbf{k}_\parallel\cdot\mathbf{R}_m), \quad (1)$$
$$g_{yy}=\frac{e^{ikr}}{r}\{k^2(1-\frac{y^2}{r^2})+\frac{ik}{r}(1-3\frac{y^2}{r^2})-\frac{1}{r^2}(1-3\frac{y^2}{r^2})\},$$

where $S_0(\mathbf{k}_\parallel,\omega)$ is the interaction lattice sum. The 0-th order reflection and transmission coefficients of the dipole array are found to be

$$r=\frac{2\pi ik}{P_xP_y}\alpha_{\text{eff}}, \qquad t=1+r.$$

The collective eigenmodes of the dipole array, corresponding to the supported surface modes, are defined by the singularities of the reflection and transmission coefficients or by zeros of the denominator $\alpha^{-1}(\omega)-S_0(\mathbf{k}_\parallel,\omega)$. In general, this condition can be satisfied only at complex frequencies $\omega=\omega_r+i\omega_i$, showing that the eigenmodes have a finite lifetime due to Ohmic losses or radiative decay [14, 32]. A real eigenvalue ω may be ideally achieved only in the limit of lossless meta-surfaces and for $k_\parallel>k$, which ensures absence of absorption and radiation.

The Wood's anomalies correspond to the frequencies at which the dipoles in the array are suppressed ($\alpha_{\text{eff}}=0$) and the array is effectively invisible and transparent to the incident radiation (r=0, t=1). This happens at the onset of the diffraction orders, for which the lattice sum diverges $S_0(\mathbf{k}_\parallel,\omega)\to\infty$. The origin of this divergence can be understood by considering a simpler model of a linear chain [9, 20, 33] of dipoles arranged along the x direction. A divergent term in this sum originates in the long-range interactions ($g_{yy}(x\to\infty,y=0)\approx k^2\exp(ikx)/x$) between dipoles.

$$S_0(k_x,\omega)\approx k^2\sum_{m\neq 0}\frac{e^{ik|x_m|}}{|x_m|}e^{-ik_xx_m}=k^2\sum_{m>0}\frac{e^{ikmP_x}}{mP_x}\{e^{-ik_xmP_x}+e^{ik_xmP_x}\}.$$

At the onset of l-th diffraction order, where $k=\pm(2\pi l/P_x+k_x)$, the lattice sum $S_0(k_x,\omega)$ grows as $\frac{k^2}{P_x}\sum_{m\neq 0}\frac{1}{m}\to\infty$.

To make the connection of Wood's anomalies with diffraction more clear, it is instructive to consider the lattice sum $S_0(\mathbf{k}_\parallel,\omega)$ in the reciprocal space [21], where it assumes the form $S_0(\mathbf{k}_\parallel,\omega)=\sum_{(l,q)}\frac{A_{(l,q)}}{k_z^{(l,q)}}+S_{0_{\text{non-singular}}}$, and diverges at the onset of (l,q) diffraction order when $k_z^{(l,q)}=\sqrt{\varepsilon(\omega/c)^2-(k_x+l\,2\pi/P_x)^2-(k_y+q\,2\pi/P_y)^2}\to 0$. Note, however, that for some diffraction orders there are no Wood's anomalies, since $A_{(l,q)}=\frac{2\pi i}{P_xP_y}[k^2-(k_y+2\pi q/P_y)^2]$ tends to zero faster than $k_z^{(l,q)}$ providing no contribution to the lattice sum at the onset of diffraction order. For example, this situation appears for the p-polarized $(0,1)$ diffraction order, which, from the physical point of view, can be explained as a result of transverse character of the long-range interaction among dipoles, which do not radiate in the far-field along the direction of their moments ($g_{yy}(x=0,y\to\infty)\sim 1/y^2$ while $g_{yy}(x\to\infty,y=0)\sim 1/x$).

2.2. Double-antenna meta-surface

The dipole model can be generalized to the case of two parallel dipoles per unit cell, corresponding to a pair of plasmonic antennas in DAM. Let us consider two point-dipoles with electric dipole moments p_1 and p_2 aligned along the y-direction and separated by a distance d along

#151537 - $15.00 USD Received 22 Jul 2011; revised 15 Sep 2011; accepted 16 Sep 2011; published 24 Oct 2011

the x-direction under an s-polarized illumination with k_y=0. Assuming the same polarizability α for both dipoles, we obtain a relation for the dipole moments in the array:

$$\begin{bmatrix} \alpha^{-1}-S_0 & -S_+ \\ -S_- & \alpha^{-1}-S_0 \end{bmatrix} \begin{bmatrix} p_1 \\ p_2 \end{bmatrix} = E_{\text{ext}} \begin{bmatrix} e^{-ik_x d/2} \\ e^{+ik_x d/2} \end{bmatrix}, \tag{2}$$

where E_{ext} is the external electric field at the center of the 0th unit cell, $S_0 = \sum_{m\neq 0} g_{yy}(\mathbf{R}_m)\exp(-i\mathbf{k}_\parallel \cdot \mathbf{R}_m)$ and $S_\pm = \sum_m g_{yy}(\mathbf{R}_m \pm \hat{x}d)\exp(-i\mathbf{k}_\parallel \cdot \mathbf{R}_m)$. The lattice sums S_0 and S_+/S_- characterize the interaction strength within and between two sub-lattices formed by p_1's and p_2's, respectively. The basis of the two electric dipoles can be changed to the more instructive basis of sub-radiant (quadrupolar) and super-radiant (dipolar) modes by the unitary transformation $p_{\text{sub}} = p_1\exp(ik_x d/2) - p_2\exp(-ik_x d/2)$ and $p_{\text{sup}} = p_1\exp(ik_x d/2) + p_2\exp(-ik_x d/2)$:

$$\begin{bmatrix} \alpha^{-1}-S_0+\Delta & i\kappa \\ -i\kappa & \alpha^{-1}-S_0-\Delta \end{bmatrix} \begin{bmatrix} p_{\text{sup}} \\ p_{\text{sub}} \end{bmatrix} = E_{\text{ext}} \begin{bmatrix} 2 \\ 0 \end{bmatrix}, \tag{3}$$

where $\Delta = -1/2[S_+\exp(ik_x d) + S_-\exp(-ik_x d)]$ accounts for the splitting caused by the interaction between the two sub-lattices. This splitting makes the sub- and super-radiant modes red-shifted and blue-shifted, respectively, with respect to the SAM's electric-dipolar resonance. The disparity in the radiative coupling of the modes, which is reflected in their names, can be seen from the rhs of Eq. (3) which shows that only the super-radiant mode can be excited by the incident field. By reciprocity, the subradiant mode is dark and cannot radiate. Note that at normal incidence the coupling between the modes $\kappa = -i/2[S_+\exp(ik_x d) - S_-\exp(-ik_x d)]$ vanishes, implying that in this particular case the sub-radiant component p_{sub} cannot be excited, either by the external field or through the coupling with the super-radiant mode p_{sup}. For oblique incidence, however, the sub-radiant mode couples with the super-radiant mode and therefore it is indirectly coupled to the external radiation.

While Eq. (3) is diagonal for normal incidence ($\mathbf{k}_\parallel$=0), this is not the case for oblique incidence. In this case there is a coupling between the super- and sub-radiant modes p_{sup} and p_{sub} which no longer represent the eigenmodes of the system. Eq. (3) can be diagonalized through an eigen-decomposition procedure using the transformation $D = 1/(1+\delta^2)[p_{\text{sup}} + i\delta p_{\text{sub}}]$ and $Q = 1/(1+\delta^2)[i\delta p_{\text{sup}} + p_{\text{sub}}]$:

$$D = \frac{1+\Delta/X}{\alpha^{-1}-(S_0-X)}E_{\text{ext}}, \tag{4a}$$

$$Q = \frac{i\kappa/X}{\alpha^{-1}-(S_0+X)}E_{\text{ext}}, \tag{4b}$$

where $\delta = (X-\Delta)/\kappa$ and $X = (\Delta^2+\kappa^2)^{1/2}$.

The physical meaning of the last transformation is to account for the hybridization of sub-radiant and super-radiant modes which takes place at oblique incidence. Since the hybridization is weak ($|\delta| \ll 1$), the modes D and Q are still dominated by super-radiant and sub-radiant components, respectively, and also have very disparate radiative coupling. It would be reasonable for these modes to be referred to as quasi super- and sub-radiant modes, however, for the sake of convenience we refer them to as dipolar and quadrupolar modes. In the special case of normal incidence, the quadrupolar mode Q coincides with the sub-radiant mode p_{sub} ($\delta = 0$) and is completely decoupled from the incident light having its lifetime limited only by the Ohmic losses. However, at finite angles, as a result of hybridization with the super-radiant component p_{sup}, it acquires a finite electric-dipolar moment and its radiative coupling and bandwidth

#151537 - $15.00 USD Received 22 Jul 2011; revised 15 Sep 2011; accepted 16 Sep 2011; published 24 Oct 2011

gradually increase. The dipolar mode D, in contrast, is always strongly radiatively coupled and hence it is spectrally broad at any incidence angle.

Comparing Eqs. (4) with their single-antenna counterpart Eq. (1), we can identify $S_D = S_0 - X$ and $S_Q = S_0 + X$ as effective lattice sums for the modified modal coefficients D and Q of the double dipole meta-molecules. Just as in the case of SAM, for DAM the modal dispersion can be obtained by tracing the poles of the denominators in Eqs. (4).

The 0-th order reflection and transmission from the array can be expressed in terms of modal amplitudes in the form

$$r = \frac{2\pi ik}{P_x P_y} p_{\text{sup}} = \frac{2\pi ik}{P_x P_y}(D - i\delta Q), \qquad t = 1 + r. \tag{5}$$

The dipole moments of the antennas in the two sub-lattices can also be written in terms of the D and Q modes as

$$p_1 = e^{-\frac{ik_x d}{2}}\{\frac{1 - i\delta}{2}(D + Q)\}, \tag{6a}$$

$$p_2 = e^{\frac{ik_x d}{2}}\{\frac{1 + i\delta}{2}(D - Q)\}. \tag{6b}$$

In order to study the optical response of the array close to the onset of a diffraction order, we consider the lattice sums in the reciprocal space which assume the form:

$$\begin{aligned} S_0 &= \sum_{(l,q)} \frac{A_{(l,q)}}{k_z^{(l,q)}} + S_{0_{\text{non-singular}}}, \\ S_\pm &= \sum_{(l,q)} \frac{A_{(l,q)}}{k_z^{(l,q)}} \exp[\mp i(k_x + \frac{2\pi l}{P_x})d], \\ \Delta &= -\sum_{(l,q)} \frac{A_{(l,q)}}{k_z^{(l,q)}} \cos(\frac{2\pi l}{P_x} d), \\ \kappa &= -\sum_{(l,q)} \frac{A_{(l,q)}}{k_z^{(l,q)}} \sin(\frac{2\pi l}{P_x} d). \end{aligned} \tag{7}$$

Here we focus on the (-1,0) order since in our case it is spectrally close to the antenna resonance. As we approach the (-1,0) Wood's anomaly, the terms containing $1/k_z^{(-1,0)}$ diverge and we can approximate the sums by retaining only these terms:

$$\begin{aligned} S_0 &\to \frac{A_{(-1,0)}}{k_z^{(-1,0)}}, \\ \Delta &\to -\frac{A_{(-1,0)}}{k_z^{(-1,0)}} \cos(\frac{2\pi}{P_x} d), \\ \kappa &\to \frac{A_{(-1,0)}}{k_z^{(-1,0)}} \sin(\frac{2\pi}{P_x} d), \\ X &\to \frac{A_{(-1,0)}}{k_z^{(-1,0)}}, \\ \delta &\to \frac{1 + \cos(2\pi d/P_x)}{\sin(2\pi d/P_x)} = \tan[\pi/2 - 2\pi d/P_x]. \end{aligned} \tag{8}$$

#151537 - $15.00 USD Received 22 Jul 2011; revised 15 Sep 2011; accepted 16 Sep 2011; published 24 Oct 2011

Note that this approximation breaks down for normal incidence, since there are two degenerate resonant terms, corresponding to (-1,0) and (1,0) diffraction orders. Away from normal incidence, where this approximation holds, the 0-th order reflection coefficient simplifies to

$$r_{\mathrm{WA}} = \frac{2\pi ik}{P_x P_y(\alpha^{-1} - S_0 + X)}[1 - \cos(\frac{2\pi d}{P_x})]. \tag{9}$$

As evident from Eq. (8), the divergent terms in $S_D = S_0 - X$ cancel out, but they are still present in $S_Q = S_0 + X$, implying that at the Wood's anomaly, the quadrupolar component vanishes (Q=0) but the dipolar component (D) remains finite, hence the reflection does not vanish as in the SAM case.

Finally, it is worthwhile noting that there is a connection between the SAM and DAM topologies. For a vanishing separation between the dipole pair ($d \to 0$), DAM reduces to a periodic array of single electric dipoles with a polarizability 2α, thus confirming the self-consistency of the generalized dipole model. As $d \to 0$, the Wood's anomalies in DAM reappear and the quadrupolar resonance disappears. At the position of the Wood's anomaly, $p_2 = -p_1$ and p_{sup}=$p_1 + p_2$=0, implying that we restore the well-know result r=0 and t=1, which also follows from Eq. (9).

2.3. Comparison between SAM and DAM

In general, one may expect a similar behavior for dipolar modes in SAM and more complex meta-molecules, such as in DAM. However, the numerical results show that in DAMs the character of interaction between antennas is substantially changed. To illustrate this, we plot side by side the transmission spectra of both SAM and DAM in Fig. 2. The SAM spectra (Fig. 2a) exhibit spectral features of two kinds. One appears as a minimum of transmission and corresponds to the coupling of the incident light to the collective dipolar mode with a dispersion $\omega_c(\mathbf{k}_\parallel)$ defined by the equation:

$$\Re\{\alpha^{-1}(\omega_c) - S_0(\mathbf{k}_\parallel, \omega_c)\} = 0. \tag{10}$$

Another one appears as a maximum of transmission, corresponding to the Wood's anomalies (shown by the color arrows in Fig. 2a and the dashed lines in Fig. 2c) of the array at the onset of the diffraction orders ($k_z^{(l,q)} = 0$). Note that this maximum never reaches unity due to the presence of the substrate. While the dipole model considered above does not capture the substrate effects, this can be accomplished by combining the model with the S-matrix formalism [34, 35]. However, the modal matching technique used here to calculate the optical response of SAM and DAM [29] rigorously considers the presence of the substrate.

For normal incidence the collective dipolar mode appears in close proximity to the electric-dipolar mode of an isolated antenna. As can be seen from Fig. 2(a,c), at larger angles it starts shifting due to "dragging" by the substrate-side (-1,0) Wood's anomaly and these two features always appear in close proximity to each other for large angles. The presence of the Wood's anomaly and its effect on the dipolar resonance are clearly related to the role of long-range interactions among meta-molecules and demonstrates the collective character of the mode [21]. Indeed, for an individual antenna the dipolar resonance corresponds to the condition $\Re\{\alpha^{-1}(\omega_0)\} = 0$, and the resonant frequency ω_0 is independent of the angle of incidence. The interaction among dipoles in the array alters the resonance position and shifts it to the new frequency ω_c defined by Eq.(10). If the resonance of the single-antenna is significantly away from the arrays Wood's anomalies, $S_0(\mathbf{k}_\parallel, \omega_c)$ is small and the resonant frequency ω_c is close to the resonance of the individual antennas. In this regime, the long-range interaction among meta-molecules is negligible and the array response is dominated by individual inclusions. However, closer to the Wood's anomaly the effect of the interaction among dipoles will result

#151537 - $15.00 USD Received 22 Jul 2011; revised 15 Sep 2011; accepted 16 Sep 2011; published 24 Oct 2011

in a dramatic change in the frequency of the collective resonance ω_c due to the large value of $S_0(\mathbf{k}_\parallel, \omega_c)$ [21].

Note that because the dipolar long-range interaction among antennas is effective only in the direction perpendicular to the antenna dipolar moment, the Wood's anomaly (and the "dragging" associated with it) appears only for *s*-polarized incidence ($k_y = 0$, $k_x \neq 0$), i.e., when the wave-vector of the incident wave lies in the *xz*-plane. For *p*-polarized incidence (k_x=0, $k_y \neq 0$), when the wave-vector lies in the *yz*-plane, the dragging effect does not appear within the framework of the dipole model.

Another effect of the periodical arrangement is the suppression of the radiative losses of the dipolar mode [21], which has been recently utilized for Surface Enhanced Infrared Absorption spectroscopy [4] and fluorescence enhancement [36, 37]. Below the light line ($k_\parallel > k$), the imaginary parts of α^{-1} and the lattice sum S_0 exactly cancel out giving rise to the formation of guided surface waves [9, 20, 10, 11, 21]. However, even above the light line, when the collective dipolar eigenmodes correspond to complex or leaky waves, the interaction results in suppression of a portion of the radiative decay of the mode and the collective dipolar resonance appears spectrally narrower as compared to the single-antenna dipolar resonance [15, 16, 17, 18, 19, 21].

Remarkably, we do not observe the expected sharp spectral features at the frequencies corresponding to the substrate-side (-1,0) Wood's anomaly in the DAM case (Fig. 2b). The expected transmission peak is absent and the spectral position of the collective dipolar mode appears to be insensitive to the angle of incidence. This is a very peculiar behavior, since one would expect that both in SAM and DAM the electric-dipolar moments of meta-molecules interact through the same dipole-dipole mechanism, and therefore should exhibit similar spectral behavior. It is also important to notice that the bandwidth of the modes in SAM and DAM is very different indicating a different extent of the suppression of the mode's radiative decay caused by a different character of the long-range interactions among meta-molecules of different topologies.

The analytical dipole model can readily describe the observed difference between SAM and DAM structures. We have shown that for SAM the expression for $S_0(\mathbf{k}_\parallel, \omega)$ diverges at the frequency corresponding to the onset of diffraction orders. This gives rise to a Wood's anomaly which appears as a peak in the transmission spectrum. In the DAM case, one would expect Wood's anomalies due to the divergence of the effective lattice sum for the electric-dipolar moment of Eq. (4), $S_D(\mathbf{k}_\parallel, \omega) = S_0(\mathbf{k}_\parallel, \omega) - X(\mathbf{k}_\parallel, \omega)$. However in DAM the diverging terms in $S_0(\mathbf{k}_\parallel, \omega)$ and $X(\mathbf{k}_\parallel, \omega)$, as can be seen from Eq. (8), cancel out exactly, resulting in the disappearance of the Wood's anomaly and eliminating the expected spectral features.

For qualitative explanation of this effect it is instructive to look at the interactions in the dipolar array in the real space. For simplicity we consider a single chain of double-antenna meta-molecules which captures all the physics of the two-dimensional structure for the particular (-1,0) *s*-polarized diffraction order. We consider one row of double-antenna meta-molecules arranged along the *x* direction. From the first equality in Eq. (2), we obtain

$$[\alpha^{-1} - (S_0 + \frac{p_2}{p_1} S_+)] p_1 = e^{-i\frac{k_x d}{2}} E_{\text{ext}}. \tag{11}$$

Now we will show that at the onset of the (-1,0) diffraction order, the effective lattice sum for the p_1's dipoles, $S_1 = S_0 + \frac{p_2}{p_1} S_+$, does not have a divergent term

$$S_1 = \sum_{m \neq 0} g_{yy}(x_m) e^{-ik_x x_m} + \frac{p_2}{p_1} \sum_m g_{yy}(x_m + d) e^{-ik_x x_m}.$$

A divergent term in this sum would have come from the long-range interactions (decaying as r^{-1}) among meta-molecules. Let us consider a DAM meta-molecule (labeled *m*) located in

#151537 - $15.00 USD Received 22 Jul 2011; revised 15 Sep 2011; accepted 16 Sep 2011; published 24 Oct 2011

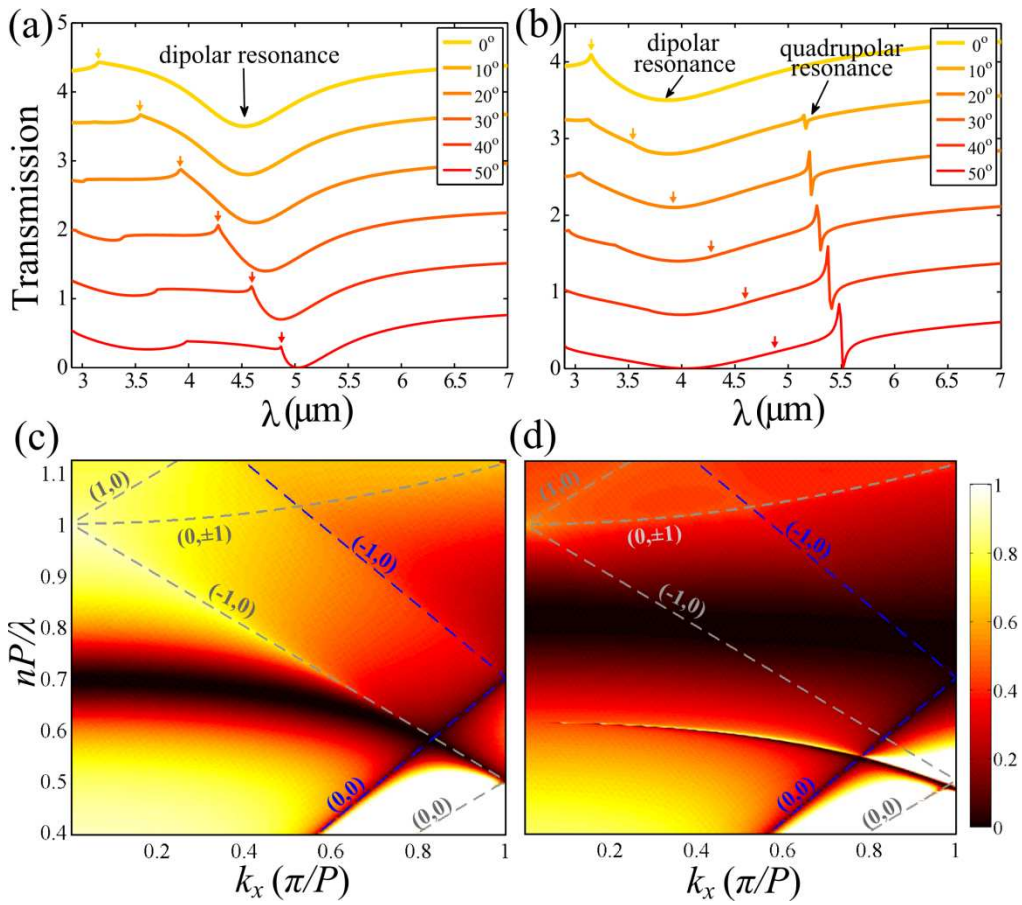

Fig. 2. Calculated transmission spectra for *s*-polarized light in (a,c) SAM and (b,d) DAM perfectly conducting antennas on CaF_2 substrate. In (a,b), color arrows indicate the spectral position of the onset of the substrate-side (-1,0) diffraction order where the Wood's anomaly for SAM is observed while for DAM it is suppressed. Offset between different curves is 0.7. In (c,d) dashed lines show spectral position of substrate-side (gray) and air-side (blue) Wood's anomalies. Structure parameters are given in Fig. 1.

the far-field from the origin. As can be seen from the expression for g_{yy} given in Eq. (1), in the far-field limit, the contribution to the lattice sum S_1 due to the interaction with the m-th meta-molecule becomes

$$g_{yy}(x_m) + \frac{p_2}{p_1} g_{yy}(x_m + d) \approx \frac{e^{ikx_m}}{x_m} + \frac{p_2}{p_1} \frac{e^{ik(x_m+d)}}{x_m + d} = \frac{e^{ikx_m}}{x_m} \{1 + \frac{p_2}{p_1} e^{ikd}\} + O(d/x_m)^2.$$

At the (-1,0) Wood's anomaly $k = \frac{2\pi}{P} - k_x$ and $\frac{p_2}{p_1} = -e^{i(k_x - 2\pi/P)d} = -e^{-ikd}$, according to Eqs. (6) and (8). Then the first term in the rhs vanishes and the contribution of the m-th unit cell to the lattice sum S_1 decays as

$$g_{yy}(x_m) + \frac{p_2}{p_1} g_{yy}(x_m + d) \approx \frac{1}{x_m^2}.$$

#151537 - $15.00 USD Received 22 Jul 2011; revised 15 Sep 2011; accepted 16 Sep 2011; published 24 Oct 2011

Thus, the interaction among the double-antenna meta-molecules decays too fast to result in a divergence in the lattice sum, which gives rise to the observed disappearance of the Wood's anomaly.

The suppression of the long-range interaction results in anomalous dispersion of the collective dipolar mode *D* in DAM. This can be clearly seen by comparing the spectral position of the minima corresponding to the collective dipolar modes in SAM and DAM transmission spectra in Figs. 2c and 2d. One can see that in the case of SAM, the dipolar mode is strongly dispersive because of "dragging" by the Wood's anomaly while in the DAM it is rather flat. In the case of SAM, the spectral position of the dipolar mode is strongly affected by the presence of the diverging lattice sum in the denominator of Eq. (1), $\alpha(\omega)^{-1} - S_0(\mathbf{k}_\parallel, \omega)$, and the mode acquires strong angular dependence. In contrast, in the case of DAM, the spatial dispersion of the mode is largely reduced, due to the cancellation of the diverging terms in the effective lattice sum $S_D(\mathbf{k}_\parallel, \omega)$.

Now we focus on the quadrupolar resonance in DAM. From Eq. (8) one can see that in this case the Wood's anomaly survives *because the effective "lattice sum"* $S_Q(\mathbf{k}_\parallel, \omega) = S_0(\mathbf{k}_\parallel, \omega) + X(\mathbf{k}_\parallel, \omega)$ *for the quadrupolar moment of the meta-molecules does diverge*. As a result we see that the spectral position of the collective quadrupolar mode is affected by the Wood's anomaly and the resonance is "dragged" to the long wavelength range at large angles (Fig. 2d). Just as in the case of the dipolar resonance in SAM, in DAM the quadrupolar resonance follows the Wood's anomaly and experiences a strong spatial dispersion.

3. Experimental results

3.1. Fabrication and optical setup

SAM and DAM arrays with the area of 400×400 μm^2 and dimensions of the unit cell given in the caption of Fig. 1 were fabricated on 0.5-mm thick CaF_2 substrates using electron beam lithography (EBL). Polymethyl methacrylate (MicroChem 950 PMMA C2) was spun at 1700 revolutions per second for 30 seconds on the substrate. A thin layer (5 nm) of chromium was deposited on the PMMA to promote conduction. This layer was etched away with chemical etchant (Transcene chromium etchant 1020AC) after exposure, before developing the sample. Desired structures were written (dosage was 300nC/cm^2 at 10pA beam current) using a Raith 50 EBL system and then developed in 1:3 MIBK:IPA developer (MicroChem) for 40s. A 3-nm thin layer of chromium was used to enhance the adhesion of the gold layer on quartz. Then an 80-nm thick layer of gold was deposited using a thermal evaporator at a base pressure of 9×10^{-7} torr. Finally, the sample was immersed in acetone for approximately one hour for liftoff. An SEM image of the fabricated DAM structure is shown in Fig. 1b. The angular-resolved transmission data were collected using a custom-made beamline based on a Fourier transform infrared (FTIR) spectrometer with the beam diameter of 300 μm. All spectra were normalized to a background of open transmission. In all cases spectra were collected at a resolution of 8 cm^{-1} and consist of 256 averaged scans.

3.2. Mid-IR spectroscopy of SAM and DAM

Experimental results for both SAM and DAM are shown in Fig. 3, which illustrates good agreement with the theoretical predictions in Fig. 2. Comparison of linear plots [Fig. 3 (a,b)] for the two designs clearly shows disappearance of the Wood's anomaly for the double-antenna case and a transmission peak at the frequency of the onset of the s-polarized (-1,0) diffraction is observed only for the case of single-antennas. The angular-resolved transmission spectra, plotted in color in Fig. 3 (c,d), confirm the expected drastic difference in the angular dependence of the spectral position of the dipolar mode in SAM and DAM. While the range of the accessible angles of incidence is limited by the experimental setup design, the dragging is still clear in

#151537 - $15.00 USD Received 22 Jul 2011; revised 15 Sep 2011; accepted 16 Sep 2011; published 24 Oct 2011

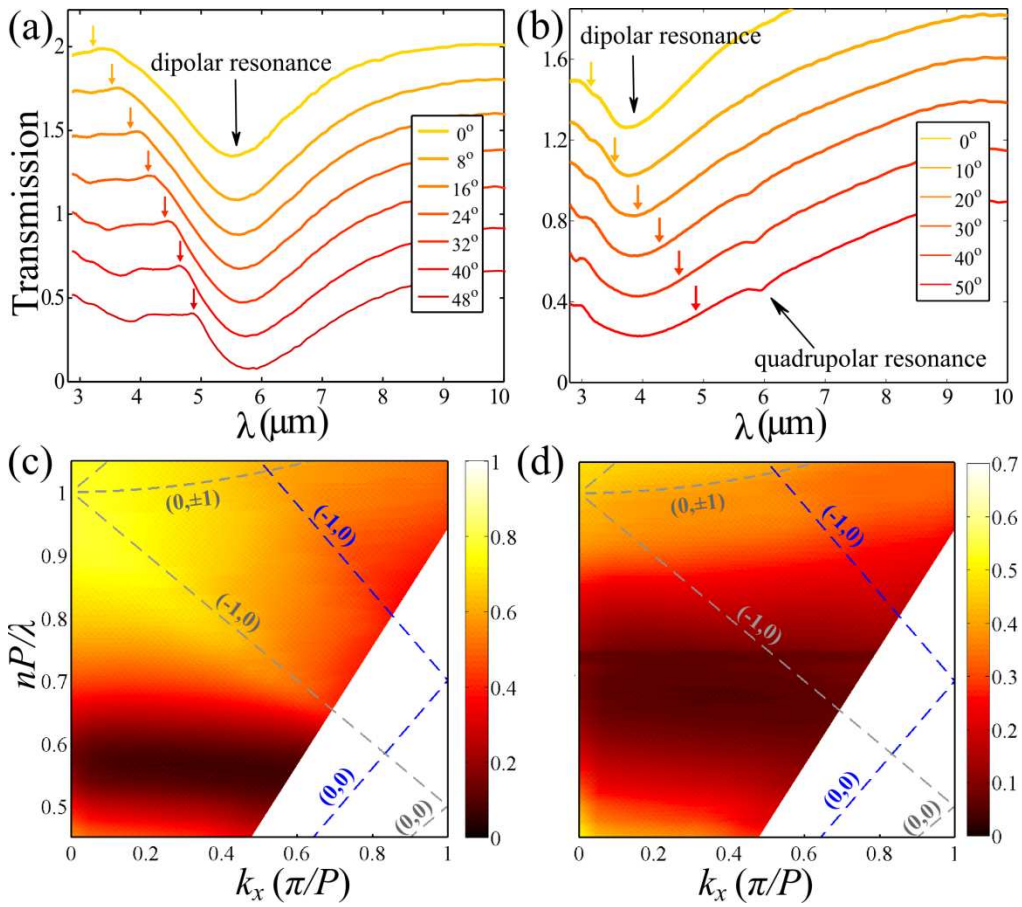

Fig. 3. Experimental *s*-polarized transmission spectra for (a,c) SAM (b,d) DAM structures made of 75-nm thick gold (Au) antennas. In (a,b) color arrows indicate the expected spectral position of the onset of the substrate-side (-1,0) diffraction order where the Wood's anomaly for SAM is observed while for DAM it is suppressed. Offset between different curves is 0.2. In (c,d) dashed lines show spectral position of substrate-side (gray) and air-side (blue) Wood's anomalies. The structure parameters are given in Fig. 1.

the SAM case at large angles. In contrast, for the DAM design, the suppression of the far-field interaction among meta-molecules makes the spectral position of the dipolar mode insensitive to the angle of incidence and it passes straight through the gray dashed line where the Wood's anomaly is expected. The change in the character of the long-range interaction also alters the lifetime of the dipolar mode which is broader for DAM.

The collective quadrupolar resonance in DAM can be seen around $\lambda = 6\ \mu m$, however it is not as pronounced as in the theoretical calculations, which is probably the result of the imperfections of the structure. Indeed, it is expected that the quadrupolar mode is more sensitive to metal roughness and disorder as compared to the dipolar mode due to its higher quality factor. Nevertheless, the experimental data clearly reveal theoretically predicted strong interaction among the quadrupolar moments of the meta-molecules. This is manifested in the transmission spectra as a dragging of the quadrupolar resonance by the Wood's anomaly. One can see that, as the frequency corresponding to the onset of the *s*-polarized substrate-side (-1,0) diffraction

#151537 - $15.00 USD Received 22 Jul 2011; revised 15 Sep 2011; accepted 16 Sep 2011; published 24 Oct 2011

order approaches the quadrupolar resonance, its spectral position red-shifts due to ”repulsion” from the Wood’s anomaly.

3.3. Near-IR spectroscopy of SAM and DAM

The results presented so far have been limited to the mid-IR frequency range where metals behave as nearly perfect conductors. However, one may expect changes in the collective behavior of the periodic meta-surfaces in the near-IR frequency range where plasmonic effects start playing an important role in light-matter interaction. To reveal any changes associated with plasmonic effects, we have to refer to previous studies of light scattering by DAM structures. In Ref. [23], a silver (Ag) DAM was compared to a split-ring resonator metamaterial, and the dimensions of meta-molecules were scaled to exhibit resonances and Wood’s anomalies in the near-IR spectral range.

The theoretical calculations, as shown in Fig. 4a, did not reveal any changes in collective behavior as compared to the mid-IR domain presented above. Again, the Wood’s anomaly is absent in the transmission spectra and the dragging effect does not exist. Therefore, there is no evidence that plasmonic effects in near-IR may result in reappearance of the far-field interaction in DAM. The only effect of finite conductivity manifests as a modification of the antennas’ polarizability and resonant frequency.

Near-IR experimental data reported in [23] for a silver DAM (fabricated by EBL on a SiO_2 substrate) confirm the theoretically predicted behavior. The experimental results are presented in Fig. 4b, and clearly show the disappearance of the Wood’s anomalies and anomalously flat dispersion of the dipolar mode caused by the cancellation of the long-range interaction between the double-antenna meta-molecules.

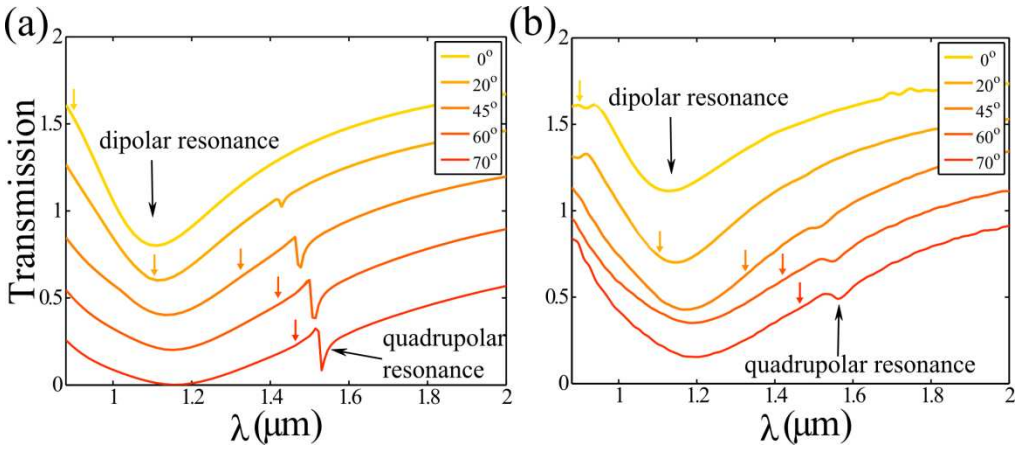

Fig. 4. Theoretical (a) and experimental (b) near-IR *s*-polarized transmission spectra for 75-nm thick plasmonic (Ag) DAM on glass (SiO_2) substrate. Vertical color arrows indicate the expected spectral position of the onset of the substrate-side (-1,0) diffraction order. The offset between different curves is 0.2. Structure parameters are $a_y = 350$ nm, $a_x = 105$ nm, $\varepsilon_{SiO_2} = 2.25$, $P_x = P_y = 600$ nm, and $d = 230$ nm.

4. Conclusion

We have both theoretically and experimentally demonstrated the importance of the topology of meta-molecules in the collective response of frequency-selective meta-surfaces. A meta-surface comprised of a periodic array of double-antenna meta-molecules was studied as an example. We

#151537 - $15.00 USD Received 22 Jul 2011; revised 15 Sep 2011; accepted 16 Sep 2011; published 24 Oct 2011

have proposed an analytical dipole model to provide a clear description of the suppression of non-local effects and long-range interactions between dipolar moments of the meta-molecules, resulting in the disappearance of the Wood's anomalies and anomalous dispersion of the collective modes of the structure. The predicted results have been experimentally confirmed in mid- and near-IR spectral domains. The discovered strong sensitivity of the spectral characteristics of collective modes envisions new approaches to design metamaterials with engineered optical properties that may avoid significant spatial dispersion effects or weaken the dependence of the response on the incidence angle.

Acknowlegments

This work was supported by the Air Force Research Laboratory and NSF CMMI-0928664 award. A.A. has been partially supported by AFOSR with the YIP award No. FA9550-11-1-0009 and by the ONR MURI grant No. N00014-10-1-0942.

#151537 - $15.00 USD Received 22 Jul 2011; revised 15 Sep 2011; accepted 16 Sep 2011; published 24 Oct 2011